

## Nonlinear refractive index of optical crystals

Robert Adair, L. L. Chase, and Stephen A. Payne

*Lawrence Livermore National Laboratory, University of California, P.O. Box 5508, Livermore, California 94550*

(Received 18 March 1988)

The nonlinear refractive indices ( $n_2$ ) of a large number of optical crystals have been measured at a wavelength near one micrometer with use of nearly degenerate three-wave mixing. The measurements are compared with the predictions of an empirical formula derived by Boling, Glass, and Owyong. This formula, which relates  $n_2$  to the linear refractive index and its dispersion, is shown to be accurate to within about 30% for materials with nonlinear indices ranging over 3 orders of magnitude. Measurements for a number of binary oxide and fluoride crystals have been analyzed under the assumption that the hyperpolarizability of the anion is much larger than that of the cation. It is found that the hyperpolarizability of oxygen varies by a factor of 10, and that of fluorine varies by a factor of 7, depending on the size of the coordinating cation. This behavior is similar to that of the linear polarizability, although the hyperpolarizability is much more sensitive than the linear polarizability to the identity of the cation. The measured halide ion hyperpolarizabilities for several alkali-halide crystals are in reasonable agreement with recent self-consistent calculations. A semiempirical model was proposed by Wilson and Curtis to account for the dependence of the linear anionic polarizability on the radius of the cation. This model also accounts quite well for the variation of the hyperpolarizability of both fluorine and oxygen, except for cation partners that have filled or unfilled  $d$ -electron shells. The nonlinear indices of a number of complex oxides (i.e., those with more than one cation) have been calculated from the partial hyperpolarizabilities deduced from the data for the binary oxides. The calculated and measured values of  $n_2$  agree to within an average error of 13%.

### I. INTRODUCTION

#### A. Background

Nonlinear-optical properties of materials have steadily increased in importance since the invention of the laser. Most attention has been focused on the second-order nonlinearity,  $\chi^{(2)}$ , of noncentrosymmetric materials because of its applications to harmonic generation and frequency shifting using parametric oscillators.<sup>1</sup> The third-order nonlinearity  $\chi^{(3)}$  has also become of increasing interest because of its effects on optical propagation of intense beams and its rapidly proliferating importance and applications in modern optical technology. Since the pioneering work of Maker and Terhune,<sup>2</sup> there have been many efforts, mostly rather limited in scope, to measure third-order nonlinearities of optical materials and to relate their nonlinear behavior to their linear refractive index and compositional and structural characteristics.<sup>3-5</sup> It is generally understood that the third-order nonlinearity at optical frequencies far below the optical band gap increases more or less monotonically with the linear refractive index. This has inspired attempts to empirically relate the third-order nonlinearity to linear-refractive-index data, although the database of  $\chi^{(3)}$  measurements used was not extensive and included mostly low-index crystals and glasses.<sup>5</sup> This work will be reviewed in the next section.

The purpose of the present work is to obtain accurate *relative* measurements of the nonlinear refractive index  $n_2$  for a wide range of optical materials. The nonlinear

refractive index is one of the simplest properties derived from  $\chi^{(3)}$ , which is a very complicated quantity in its most general form.  $n_2$  is defined by<sup>6</sup>

$$n = n_0 + n_2 \langle E^2 \rangle, \quad (1)$$

where  $n_0$  is the linear refractive index and  $E$  is the applied optical electric field. For linearly polarized light in an isotropic medium or light polarized along a cube axis in a cubic crystal,  $n_2$  is related to  $\chi^{(3)}$  by<sup>7</sup>

$$n_2 = \frac{12\pi}{n_0} \chi_{1111}^{(3)}. \quad (2)$$

The nonlinear index is an important consideration in the design of high-power lasers and optical systems. Spatial intensity fluctuations in the wavefront of a laser beam passing through a medium grow exponentially with the nonlinear phase shift that is proportional to  $n_2$ .<sup>7</sup>

#### B. Microscopic and empirical models for $n_2$

The nonlinear refractive index is determined by several physical mechanisms, acting on a broad range of time scales. It is therefore necessary to be explicit about the contributing mechanisms in a particular experiment. The various contributions to  $n_2$  are<sup>8,9</sup>

$$n_2 = n_2(\text{electronic}) + n_2(\text{vibrational}) \\ + n_2(\text{electrostriction}) + n_2(\text{thermal}). \quad (3)$$

The response times of these various contributions can be estimated from simple arguments. The electronic and vi-

brational response times can be obtained from the frequencies of optical transitions involving the bound electrons and lattice vibrations; these are  $\sim 10^{-15}$  and  $10^{-13}$  s, respectively. The electrostrictive response time is roughly equal to the time required for an acoustic deformation to travel across the diameter of the optical beam, or about  $10^{-8}$  s under our experimental conditions. Thermal diffusion time scales are even longer, and depend on the thermal properties of the medium. In the propagation of nanosecond laser pulses through a medium only the first two of the mechanisms in Eq. (3) are active. These are also the only two mechanisms that contribute to our measured values of  $n_2$ .

Calculations of  $n_2$  are very difficult because of the high order of perturbation theory involved and the consequent need for accurate wave functions and energies for a large number of excited states. Progress has been made, however, since the early work by Boyle *et al.* on third-order nonlinearities in helium.<sup>10</sup> Recently, self-consistent calculations were done on alkali halide crystals using the local-density approximation;<sup>11,12</sup> we shall discuss these later. For the majority of the crystals that we have measured, however, there are no first-principles calculations available. We shall therefore base most of the discussion of our results on some empirical concepts and approximations with the aim of investigating their possible validity. It is possible that this will lead to some insight into the most promising directions of future theoretical work on the third-order nonlinearity.

One of the earliest concepts employed to model the linear-optical response of condensed matter is the polarization of the constituent atoms, ions, or molecules. Tessman *et al.* showed that this approach leads to reasonably consistent values for the polarizabilities of the alkali and halide ions calculated from the refractive indices of alkali halide crystals.<sup>13</sup> This concept can be formally generalized to the third-order nonlinearity by defining the hyperpolarizability  $\gamma_i$  of a microscopic constituent in analogy with the linear polarizability  $\alpha_i$ . The polarization of such a constituent is defined as

$$p_i = \alpha_i E_i + \gamma_i E_i^3 / 6. \quad (4)$$

Here,  $E_i$  is the local electric field. Wang<sup>4</sup> obtained a simple empirical relationship between the  $\alpha$  and  $\gamma$  for hydrogenic atoms by simplifying the perturbation-theory expression for  $\gamma$  in the limit of an optical frequency much lower than any optical transitions to excited states. This relation states that  $\gamma = k\alpha^2$ , where  $k$  is inversely proportional to the average excitation energy of optical transitions to excited states that have a dominant influence on the hyperpolarizability. Boling, Glass, and Owyong<sup>5</sup> (BGO) showed that this relation can be generalized to a multielectron atom or ion. They wrote the nonlinear refractive index as

$$n_2 = \frac{f^4 \pi}{2n} \sum_i N_i \gamma_i, \quad (5)$$

where  $N_i$  is the number density of species  $i$ , and  $f$  is the local-field correction factor, which they took to be the Lorentz local field  $f = (n^2 + 2)/3$ . They assumed that

one constituent had a hyperpolarizability that was much larger than any others and modeled its linear-optical response by a single harmonic oscillator whose frequency could be related to the dispersion of the linear refractive index. From this ansatz they deduced the empirical expression for  $n_2$ ,<sup>5</sup>

$$n_2 = \frac{K(n_d - 1)(n_d^2 + 2)^2}{v_d \left[ 1.517 + \frac{(n_d^2 + 2)(n_d + 1)}{6n_d} v_d \right]^{1/2}} \times 10^{-13} \text{ esu}, \quad (6)$$

where  $n_d$  is the linear refractive index at the  $d$  line of He at 5875.6 Å and  $v_d$  is the Abbe number, which is the reciprocal of the wavelength dispersion of the linear refractive index of the medium at this wavelength.  $K$  is an empirical factor that they suggested might be reasonably constant for a group of related materials. This formula has been fairly successful in predicting the nonlinear refractive indices of many low-index crystals and glasses,<sup>5,14-19</sup> and there are some indications that it may apply to high-index semiconductors as well.<sup>20</sup>

Recently, Johnson *et al.*<sup>12</sup> have done self-consistent calculations of the effective ionic hyperpolarizabilities of alkali and halide ions in alkali halide crystals using the local-density approximation (LDA) with either *ab initio* or spherically averaged pseudopotential methods. They found that the hyperpolarizabilities of the anions  $F^-$ ,  $Cl^-$ ,  $Br^-$ , and  $I^-$  are much larger than those of the cations, and they vary by severalfold depending on the identity of the coordinating cation. Furthermore, they found that the variation of the hyperpolarizability is much larger than that of the linear polarizability. In the face of this evidence, the assumption of ionic hyperpolarizabilities that are relatively independent of the identity of the counterions is clearly untenable as a starting point. An alternative approach would be to assume that the basic constituents whose hyperpolarizabilities are summed together in Eq. (5) are cation-anion pairs, which includes the "bonds" between such pairs. The  $\gamma_i$  are therefore defined as variable anion hyperpolarizabilities, which are assumed to include both the interionic and intraionic contributions to the nonlinear polarization. Obviously, this simple assumption does not allow for the fact that each anion or cation of an ionic crystal may be coordinated by several ligands, which are not necessarily identical. Also, the geometric character of the coordination may vary from crystal to crystal or from site to site in a given crystal. One of the goals of our experiments is to investigate the extent to which such a concept is useful.

These models all treat  $\chi^{(3)}$  as a scalar quantity, when it is, of course, a tensor. For cubic materials there are three independent components,  $\chi_{1111}^{(3)}$ ,  $\chi_{1122}^{(3)}$ , and  $\chi_{1221}^{(3)}$ . For a linearly polarized beam propagating along [001], polarized at an angle  $\Theta$  relative to [100], the effective  $\chi^{(3)}$  may be written as<sup>2</sup>

$$\chi^{(3)}(\Theta) = (2\chi_{1122}^{(3)} + \chi_{1221}^{(3)}) + (\chi_{1111}^{(3)} - 2\chi_{1122}^{(3)} - \chi_{1221}^{(3)}) \left[ \frac{\cos^2(2\Theta) + 1}{2} \right] \quad (7)$$

for cubic crystals having space-group symmetry  $432$ ,  $43m$ , or  $m3m$  (such as  $\text{NaCl}$ ,  $\text{CaF}_2$ , and  $\text{CsCl}$ , respectively). When all of the excitation frequencies are far below one- and two-photon electronic resonances, we may use Kleinman symmetry to simplify Eq. (7):

$$\chi_{1122}^{(3)} = \chi_{1221}^{(3)}, \quad (8)$$

and therefore,

$$\chi^{(3)}(\Theta) = 3\chi_{1122}^{(3)} + (\chi_{1111}^{(3)} - 3\chi_{1122}^{(3)}) \left[ \frac{\cos^2(2\Theta) + 1}{2} \right]. \quad (9)$$

We shall make use of these expressions to obtain  $\chi_{1122}^{(3)}/\chi_{1111}^{(3)}$  for cubic crystals from our measurements of the polarization anisotropy of  $n_2$ . One might expect to be able to account for the anisotropy of  $\chi^{(3)}$  by considering an anisotropic hyperpolarizability for the bond between two atoms or ions. It is easily shown that the simplest notion, a one-dimensional bond between atom or ion pairs, does not account for the anisotropy of  $\chi^{(3)}$  for the simplest ionic or covalent cubic materials. It is therefore necessary to employ at least three independent tensor components of the bond hyperpolarizability, although only two of these are independent under the conditions where Eq. (8) is valid.

## II. EXPERIMENTAL METHOD AND SETUP

Measurements of the nonlinear refractive index were performed using the technique of nearly degenerate three-wave mixing (TWM) that we employed previously for glasses.<sup>19</sup> Since the experimental details were reported in Ref. 19, only the most basic and important information will be repeated here. The experimental setup is shown in Fig. 1. In the TWM method the  $1.064\text{-}\mu\text{m}$  beam (frequency  $\omega_1$ ) is combined with a  $1.071\text{-}\mu\text{m}$  beam (frequency  $\omega_2$ ), produced by a Raman-shifted dye laser, to generate the frequency  $2\omega_1 - \omega_2$ , using a collinear geometry for the incident and signal beams. The frequency offset  $\Delta = \omega_1 - \omega_2 = 60\text{ cm}^{-1}$  gives a coherence length for the mixing of about 10 cm, which allows the use of samples up to 1-cm thickness. Mixing is done in two nearly identical focal regions, one of which contains the sample to be measured, and the other is a reference arm containing a cell of  $\text{CS}_2$ . The signals are separated from the input waves with a double monochromator and are detected by separate photomultiplier tubes with S-1 spectral response. A two-channel gated integrator records the sample and reference signals, which are input to a computer. The sample signal is normalized by dividing it by the reference signal for each laser pulse in order to correct for fluctuations in the input laser beams. The  $n_2$  value of the sample is obtained by substituting a standard material with known  $n_2$  into the sample arm, and the magnitudes of the normalized signals for the sample and standard are used to calculate  $n_2$  for the sample from the formula

$$[\chi_{1111}^{(3)}]_s = [\chi_{1111}^{(3)}]_c \left[ \frac{I_s}{I_c} \right]^{1/2} \left[ \frac{n_s}{n_c} \right]^2 \frac{\ell_c}{\ell_s} C^2, \quad (10)$$

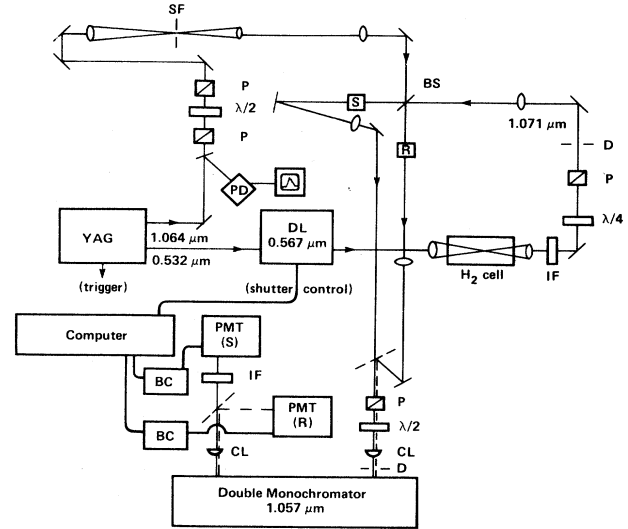


FIG. 1. Experimental setup used to measure the nonlinear refractive index. DL, dye laser; IF, interference filter; P, polarizer; D, diaphragm; BS, beamsplitter; S, sample; CL, cylindrical lens; PD, photodiode; SF, spatial filter; R, reference cell; BC, boxcar integrator; PMT, photomultiplier tube.

where  $I_s$  and  $I_c$  are the normalized signals for the sample and calibration standard, respectively,  $\ell_s$  and  $\ell_c$  are their lengths,  $n_s$  and  $n_c$  their refractive indices, and  $C^2$  corrects for differences in their surface reflectivities. Following the procedure used for our measurements of glasses, we have calibrated our "standard" sample with the average of the nonlinear refractive indices of seven glass samples measured by time-resolved interferometry by Milam *et al.*<sup>15-18</sup>

Although these relative measurements of  $n_2$  do not require a knowledge of the intensities and spatial and temporal distributions of the laser sources, there are still some possible sources of error that must be avoided. First, the use of a finite frequency difference  $\Delta$  may result in the measurement of only a partial contribution to  $n_2$  arising from the Raman-active lattice vibrations. This is most likely to be a problem with materials with very low-lying Raman-active vibrations. By varying the frequency difference  $\Delta$ , we have investigated the dispersion of the signal from a sample of lead glass,<sup>21</sup> which has vibrational excitations extending down below  $100\text{ cm}^{-1}$ . The results, shown in Table I, demonstrate that there is no dispersion to within the experimental accuracy of about 5%. Also shown in Table I are similar data for  $\text{CS}_2$ , which shows the expected dispersion from molecular reorientation.<sup>22</sup> Since all of the crystals that we have investigated in this work have no Raman-active vibrations below about  $150\text{ cm}^{-1}$ , the effects resulting from the finite value of  $\Delta$  will be even less than those expected for the lead glass. Self-focusing is a second source of error; its effects would be most severe in high-index materials, such as the lead glass. Table II shows the results of  $n_2$  measurements on the SF-58 glass as a function of laser intensity. Even at intensities near the self-focusing thresh-

TABLE I. Measured values of  $n_2$  as a function of frequency shift.

$\Delta = \omega_1 - \omega_2$ ( $\text{cm}^{-1}$ )	$n_2$ ( $10^{-13}$ esu)	
	SF-58	CS <sub>2</sub>
63.5	11.2	13.8
32.3	12.2	26.8
19.8	10.8	32.8
9.8	11.2	48.6

old for this material, our measurements are independent of laser power, so we conclude that self-focusing does not affect our measurements.

The samples employed in this work were a few mm thick. Their surfaces were polished parallel to within about  $0.3^\circ$ , which was necessary to avoid extensive realignment between insertion of the sample and standard. Measurements were repeated several times by successive interchange of the unknown and the standard. Different portions of the sample were measured each time to avoid systematic errors due to sample quality and surface finish. Many samples were measured on different days with no noticeable changes. Based on this reproducibility, we believe that the accuracy of relative  $n_2$  measurements is better than 5% for nearly all of the samples measured. Some materials (KF, KCl, NaBr, KBr, CaO, and SrO) had marginal optical quantity, and the estimated errors are on the order of 15%.

### III. EXPERIMENTAL RESULTS

Before discussing the results, it is important to review our choice of calibration standard and compare our experimental approach with those used by previous investigators. Time-resolved interferometry (TRI) is a direct method that has been employed to measure  $n_2$ .<sup>15-18</sup> The advantage of TRI is that it automatically satisfies the condition  $\Delta=0$  to within the bandwidth of the laser pulse. This method is, however, very difficult and requires large samples of excellent optical quality. Measurements of  $\chi^{(3)}$  using TWM have also made use of the absolute Raman cross sections of benzene or calcite as the nonlinear calibration standard.<sup>2,23-25</sup> These measurements must be made with a large value of  $\Delta \sim 1000 \text{ cm}^{-1}$ , which is too large to include the vibrational contribution to  $\chi^{(3)}$  in most crystals and glasses. Also, careful phase-matching geometries involving the unknown and standard materials are required. Recently, degenerate

TABLE II. Measured values of  $n_2$  as a function of intensity for SF-58 lead glass.

Laser power (kW) at $1.064 \mu\text{m}^a$	Measured $n_2$ ( $10^{-13}$ esu)
250	11.6
75	11.2
50	12.1
12	11.3

<sup>a</sup> The critical power for self-focusing is  $P_{\text{crit}} = c\lambda^2/32\pi^2 n_2 = 94 \text{ kW}$ .

four-wave mixing was used to measure  $n_2$  in glasses and some crystals.<sup>26</sup> This method is sensitive to thermal gratings and free-carrier gratings and is difficult if bulk or surface elastic scattering is appreciable. A fourth method involves the measurement of self-focusing, either by its direct effects on the far-field beam profile, or by measured optical damage thresholds.<sup>27</sup> The same problems arising in degenerate four-wave mixing, as well as the difficulty of defining the optical damage threshold, affect the self-focusing method. In order to avoid these difficulties, we have chosen to employ the nearly degenerate TWM method, which is easier to perform and interpret and less demanding of sample size and quality than any of these other approaches. We are also able to utilize many of the previous TRI measurements as a collective calibration standard. For a suitably small value of  $\Delta$  the TWM measurements should be equivalent to TRI, and the experiments discussed in the preceding section verify that the value of  $\Delta = 60 \text{ cm}^{-1}$  that we employed satisfies this condition. This choice of a calibration standard may, however, lead to errors in the absolute  $n_2$  values, since any persistent error in the calibration set is incorporated into our results.

An assessment of the uncertainty of the reference standard may be made by comparing our measurements with those obtained by the other methods. A comparison of results for selected materials is shown in Table III. The data in this table were not intended to be comprehensive, but rather to compare several different experimental techniques and standards in experiments that have a significant overlap with the materials studied in our own work. For a thorough review of previous  $n_2$  measurements, see Ref. 7. Of the listed materials measured by TRI, only fused silica was included from among the set of glasses that were used for calibration (see Ref. 19). (The crystals were not used for calibration since their orientations were unknown in the TRI experiments.) Our measurements are in good *relative* agreement with TRI for the crystals in Table III. The third column in Table III lists the results of Maker and Terhune,<sup>2</sup> who used a setup similar to ours with collinear phase matching and a large value of  $\Delta$  equal to the  $992\text{-cm}^{-1}$  vibration of benzene, which was the calibration medium. These results are consistently larger than ours by a factor of 2. The other TWM results reported by Levenson and co-workers,<sup>23-25</sup> which are based on calcite as a standard, are roughly a factor of 3 larger than ours, except for  $\text{CdF}_2$ . The *relative* values obtained by these previous investigations are, however, in good agreement with ours. The last column of Table III lists the absolute measurements of Smith *et al.*,<sup>27</sup> who extracted  $n_2$  from optical damage data in the presence of self-focusing. These measurements are less direct than the others because of the uncertain role that self-focusing plays in bulk optical damage.

We believe that the differences between our values and those obtained using TWM with benzene or calcite as the calibration standard are real and reflect a disagreement in the calibration standards. This is not unlikely since this is the first extensive comparison of  $n_2$  values obtained using the time-resolved-interferometry and Raman cross-section standards. Despite this uncertainty in the abso-

TABLE III. Comparison of work with previously published results.

Sample	Measured <sup>a</sup> $n_2$ ( $10^{-13}$ esu)						PDF <sup>h</sup> 1.06 $\mu\text{m}$
	TWM <sup>b</sup>	TRI <sup>c</sup>	TWM <sup>d</sup>	TWM <sup>e</sup>	TWM <sup>f</sup>	TWM <sup>g</sup>	
	1.06 $\mu\text{m}$ 1.07 $\mu\text{m}$	1.06 $\mu\text{m}$	0.693 $\mu\text{m}$ 0.746 $\mu\text{m}$	0.575 $\mu\text{m}$ 0.610 $\mu\text{m}$	0.575 $\mu\text{m}$ 0.592 $\mu\text{m}$	0.560 $\mu\text{m}$ 0.590 $\mu\text{m}$	
LiF	0.26	0.35	0.54			0.92	2.4
NaF	0.34	0.43					0.9
NaCl	1.59		3.2				6.5
NaBr	3.26						9.6
KCl	2.01		4.8				3.3
KBr	2.93		7.3				14.2
CaF <sub>2</sub>	0.43	0.65	0.92	1.13	1.1	1.46	2.8
SrF <sub>2</sub>	0.50	0.60		1.15	1.4		
CdF <sub>2</sub>	3.95	1.46		3.50	3.58		
BaF <sub>2</sub>	0.67	1.0		2.13	1.8		
LaF <sub>3</sub>	1.4 (av)	1.51					
CeF <sub>3</sub>	1.3 (av)	1.55					
Al <sub>2</sub> O <sub>3</sub>	1.25 (av)						
fused SiO <sub>2</sub>	0.85	0.95	1.8			2.4	
Y <sub>3</sub> Al <sub>5</sub> O <sub>12</sub>	2.7 (av)					4.5	3.5
MgO	1.61		3.3				

<sup>a</sup> TWM denotes three-wave mixing, TRI time-resolved interferometry, and PDF power-dependent focus.

<sup>b</sup> This work. This is the  $\chi_{111}^{(3)}$  component unless otherwise noted.

<sup>c</sup> References 15 and 17.

<sup>d</sup> Corrected values from Ref. 2 as cited in Ref. 28.

<sup>e</sup> Reference 23.

<sup>f</sup> Reference 24.

<sup>g</sup> Reference 25.

<sup>h</sup> Reference 27.

lute values, our relative values of  $n_2$  are believed to be accurate to better than 15% based on the reproducibility and scatter of our data.

Our measurements for all of the crystal samples are presented in Table IV. The material and polarization geometry are listed in column 1. Columns 2 and 3 give linear-index data that are useful for relating  $n_2$  to the hyperpolarizability,  $\gamma$ , and for calculating  $n_2$  from empirical models. The measured values of  $n_2$  are given in column 4. It has often been assumed that  $n_2$  increases roughly with the linear index  $n$ . Figure 2 illustrates that there is indeed a general trend of this type, but materials with identical linear indices can have values of  $n_2$  differing by up to a factor of 10. The assumptions on which the BGO model is based suggest that an additional parameter involved in the correlation between  $n$  and  $n_2$  is the magnitude of the average excitation energy of excited intermediate states.<sup>5</sup> This is incorporated into the BGO model in the form of the Abbe number, which is related to the dispersion of the linear index. The  $n_2$  values calculated from the BGO formula [Eq. (6)] are given in column 5 of Table IV. A graphic comparison of the measured and calculated values is illustrated in Fig. 3, which is a logarithmic plot of our measurements versus the predicted values from the BGO formula. The calculations were done using the empirical constant  $K=68$ , which was determined by a best fit to low-index glasses and fluoride crystals.<sup>5,15-18</sup> For perfect agreement, the plotted points

would fall on the solid line. With a few exceptions, the agreement is good for halide and many oxide crystals. Most of the oxide crystals, however, fall below the line, and a different value of the constant,  $K=48$ , represented by the dashed line, fits the entire set of data much better. The largest errors are for oxides of the sixfold-coordinated, high-valence transition-metal cations like Ti<sup>4+</sup>, Zr<sup>4+</sup>, and W<sup>6+</sup>, which fall below even the  $K=48$  line by about 40%. Overall, the BGO expression does quite well for a very wide range of transparent materials with nonlinear indices varying by over 3 orders of magnitude. A comparison of Figs. 2 and 3 confirms that dispersion, represented by the Abbe number, is a very necessary parameter for relating  $n_2$  to the linear index. Another possibly important ingredient in such a parameterization is the form of the local-field correction, which appears to the fourth power in Eq. (5). This will be discussed in the next section.

A comparison of the measured and calculated values of  $n_2$  for light polarized along different crystalline axes in strongly anisotropic materials is also of interest. If the refractive index and its dispersion are known for light polarized along different axes, one can formally calculate the value of  $n_2$  for each polarization. For potassium dihydrogen phosphate (KDP) and CaCO<sub>3</sub> the BGO formula predicts quite substantial differences between ordinary ( $o$ ) and extraordinary ( $e$ ) polarizations, whereas there are little or no differences in the measured values.

TABLE IV. Nonlinear- and linear-refractive-index data for all crystals studied in this work. (*o* denotes ordinary, *e* extraordinary.)

Sample	Linear-index data		Nonlinear-index data	
	<i>n</i> (1.06 $\mu\text{m}$ )	Abbe number $\nu_d$	Measured $n_2$ ( $10^{-13}$ esu)	Calculated $n_2$ ( $10^{-13}$ esu)
LiF[100]	1.3866 <sup>a</sup>	98.0	0.26	0.40
NaF[100]	1.3213 <sup>a</sup>	85.2	0.34	0.38
KF[100]	1.3583 <sup>a</sup>	97.9	0.75	0.36
NaCl[100]	1.5312 <sup>a</sup>	42.9	1.59	2.28
KCl[100]	1.4792 <sup>a</sup>	44.1	2.01	1.84
NaBr[100]	1.6228 <sup>a</sup>	31.7	3.26	4.74
KBr[100]	1.5435 <sup>a</sup>	33.7	2.93	3.41
MgF <sub>2</sub> ( <i>o</i> )	1.3735 <sup>b</sup>	104.9	0.25	0.34
CaF <sub>2</sub> [100]	1.4285 <sup>c</sup>	95.1	0.43	0.49
SrF <sub>2</sub> [100]	1.4328 <sup>b</sup>	93.9	0.50	0.50
CdF <sub>2</sub> [100]	1.56 <sup>d</sup>	61.0	3.95	1.37
BaF <sub>2</sub> [100]	1.4682 <sup>b</sup>	81.8	0.67	0.70
LaF <sub>3</sub> ( <i>o</i> )	1.60 <sup>b</sup>	57.0	1.4	1.78
CeF <sub>3</sub> ( <i>o</i> )	$\sim 1.6^c$		1.3	
AgCl (polycryst.)	2.020 <sup>b</sup>	21.2	23.3	23.0
MgO[100]	1.72 <sup>c</sup>	53.4	1.61	2.8
CaO[100]	1.83 <sup>c</sup>		5.20	
SrO[110]	1.81 <sup>c</sup>		5.07	
ZnO ( <i>e</i> )	1.96 <sup>c</sup>	11.6	23.0	57.6
ZnO ( <i>o</i> )	1.99 <sup>c</sup>	12.3	25.0	45.0
Al <sub>2</sub> O <sub>3</sub> ( <i>o</i> )	1.75 <sup>c</sup>	71.8	1.23	1.9
Al <sub>2</sub> O <sub>3</sub> ( <i>e</i> )	1.75 <sup>c</sup>	75.2	1.30	1.8
Ga <sub>2</sub> O <sub>3</sub>	1.96 <sup>b</sup>		5.80	
Y <sub>2</sub> O <sub>3</sub>	1.92 <sup>a</sup>	37.5	5.33	7.2
Er <sub>2</sub> O <sub>3</sub>	1.96 <sup>f</sup>		4.53	
SiO <sub>2</sub> (fused)	1.4496 <sup>c</sup>	67.8	0.85	0.83
SiO <sub>2</sub> (quartz) ( <i>o</i> )	1.5342 <sup>c</sup>	71.6	1.12	1.06
SiO <sub>2</sub> (quartz) ( <i>e</i> )	1.5429 <sup>c</sup>	70.1	1.16	1.13
TiO <sub>2</sub>	2.48 <sup>b</sup>	9.8	55.8	189
ZrO <sub>2</sub>	2.12 <sup>b</sup>	35.8	5.8	12.6
BeAl <sub>2</sub> O <sub>4</sub>	1.73 <sup>b</sup>	72.5	1.46	1.74
MgAl <sub>2</sub> O <sub>4</sub>	1.72 <sup>b</sup>	60.6	1.50	2.3
CaMgSi <sub>2</sub> O <sub>6</sub>	1.67 <sup>g</sup>		1.73	
YAlO <sub>3</sub> ( $\gamma$ )	1.933 <sup>b</sup>	51.2	3.37	4.88
Y <sub>3</sub> Al <sub>5</sub> O <sub>12</sub> (YAG)	1.822 <sup>b</sup>	52.4	2.7	3.6
Gd <sub>3</sub> Sc <sub>2</sub> Al <sub>3</sub> O <sub>12</sub> (GSAG)	1.891 <sup>h</sup>	48.0	4.0	5.6
Gd <sub>3</sub> Sc <sub>2</sub> Ga <sub>3</sub> O <sub>12</sub> (GSGG)	1.943 <sup>i</sup>	37.3	5.5	8.0
Gd <sub>3</sub> Ga <sub>5</sub> O <sub>12</sub> (GGG)	1.945 <sup>b</sup>	37.6	5.8	8.0
Y <sub>3</sub> Ga <sub>5</sub> O <sub>12</sub> (YGG)	1.912 <sup>j</sup>	40.0	5.2	5.8
La <sub>3</sub> Lu <sub>2</sub> Ga <sub>3</sub> O <sub>12</sub> (LLGG)	1.930 <sup>i</sup>	36.4	5.8	8.2
SrTiO <sub>3</sub>	2.31 <sup>c</sup>	13.6	26.7	83.0
CaCO <sub>3</sub> ( <i>o</i> )	1.6425 <sup>c</sup>	47.6	1.11	2.7
CaCO <sub>3</sub> ( <i>e</i> )	1.4795 <sup>c</sup>	76.8	0.83	0.79

The situation is reversed for LAP (*L*-arginine phosphate) for which little anisotropy is predicted for  $n_2$ , but a substantial amount is observed. These results show that the BGO formula provides unreliable predictions of the anisotropy of  $n_2$ .

#### IV. DISCUSSION

##### A. Hyperpolarizabilities of ions in crystals

In the preceding section we showed that the value of  $n_2$  can be calculated with reasonable accuracy solely on

the basis of linear-refractive-index data using the BGO formula. It would be of interest, however, to be able to estimate  $n_2$  for crystals, or structural units of crystals, for which neither linear- nor nonlinear-optical measurements have been performed. This goal requires the development of a fundamental understanding of the basic mechanism from which the nonlinear index arises.

The problem of understanding the hyperpolarizability involves many of the same issues that have confronted researchers for decades concerning the basis for the linear polarizability.<sup>40</sup> We now discuss this point in detail. The most widely used approach to the polarizability of ionic

TABLE IV. (Continued).

Sample	Linear-index data		Nonlinear-index data	
	$n$ (1.06 $\mu\text{m}$ )	Abbe number $\nu_d$	Measured $n_2$ ( $10^{-13}$ esu)	Calculated $n_2$ ( $10^{-13}$ esu)
$\text{KH}_2\text{PO}_4$ (o)	1.4598 <sup>c</sup>	70.9	0.72	0.85
$\text{KH}_2\text{PO}_4$ (e)	1.4938 <sup>c</sup>	56.6	0.78	1.35
$\text{K}(\text{TiO})\text{PO}_4$ (x + y)	1.74 <sup>k</sup>	23.5	5.73	10.0
L-arginine phosphate (y)	1.559 <sup>k</sup>	47.5	1.87	2.14
L-arginine phosphate (x + z)	1.51 <sup>k</sup>	50.0	3.04	2.0
$\text{KTaO}_3$	2.25 <sup>b</sup>		29.0	
$\text{CaWO}_4$ (o)	1.89 <sup>b</sup>	30.0	4.2	10.4
$\text{CaWO}_4$ (e)	1.91 <sup>b</sup>	28.0	5.6	12.0
$\text{ZnS}$ (e)	2.29 <sup>b</sup>	15.5	49.3	64.0
$\text{ZnS}$ (o)	2.29 <sup>b</sup>	15.5	47.3	64.0
$\text{CdS}$ (e)	2.34 <sup>c</sup>	3.8	283.0	643.0
$\text{CdS}$ (o)	2.33 <sup>c</sup>	4.4	304.0	494.0

<sup>a</sup> Reference 29.<sup>b</sup> Reference 30.<sup>c</sup> Reference 31.<sup>d</sup> Reference 32.<sup>e</sup> Reference 33.<sup>f</sup> Reference 34.<sup>g</sup> Reference 35.<sup>h</sup> Reference 36.<sup>i</sup> Reference 37.<sup>j</sup> Reference 38.<sup>k</sup> Reference 39.

crystals is the simple ionic polarizability model, whereby the polarizability of a unit cell of a medium,  $\alpha_c$ , is assumed to be determined by the sum of the contributions from the positively and negatively charged constituents,<sup>13</sup>

$$\alpha_c = \sum_i (N_i^- \alpha_i^- + N_i^+ \alpha_i^+), \quad (11)$$

where  $N_i^+$  and  $N_i^-$  are the numbers of each ion per unit cell. The work of Tessman, Kahn, and Shockley<sup>13</sup> showed that a single table of ionic polarizabilities (e.g., for  $\text{F}^-$ ,  $\text{Cl}^-$ ,  $\text{Li}^+$ ,  $\text{Na}^+$ , etc.) could account for the polarizabilities of all the alkali halides. In this work, however, serious problems with the model were recognized. For instance, the  $\alpha^-$  values were found to have only limited transferability to the other halide crystals, such as  $\text{MgCl}_2$ ,

and, for the case of the oxygen ion, it was concluded that a unique value of  $\alpha^-$  simply could not be established. A particularly insightful result in this classic article involved a brief demonstration that the polarizability of  $\text{O}^{2-}$  can be shown to increase monotonically with the volume per oxygen ion. It should be noted that this can also be interpreted as a correlation with the radius of the coordinating cation, although the cations with  $d^{10}$  outer shells or low-lying empty  $d$  shells given anomalously high oxygen polarizabilities.

Alternative models of the linear refractive index have

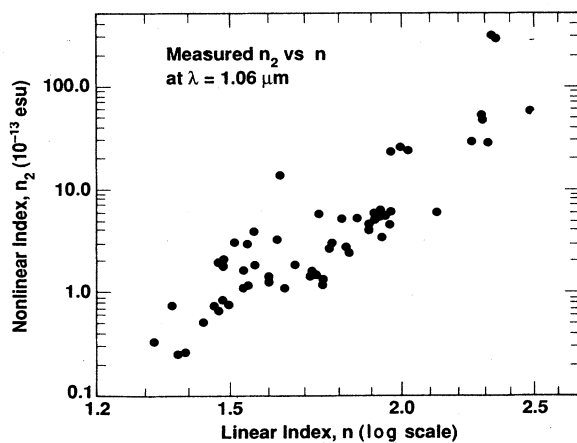


FIG. 2. Measured values of the nonlinear refractive indices of crystals plotted on a logarithmic scale as a function of their linear refractive indices.

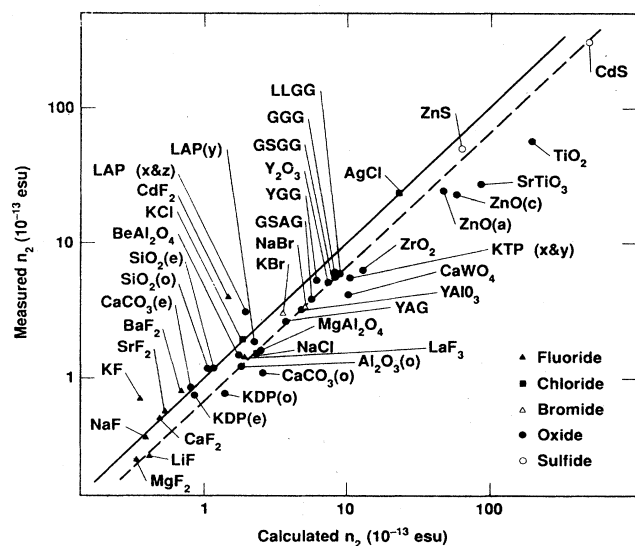


FIG. 3. Measured nonlinear refractive indices of optical crystals vs the values of  $n_2$  calculated from the BGO formula [Eq. (6)], using  $K = 68$  (solid line) and  $K = 48$  (dashed line).

taken numerous paths since this early work. One approach is that of Pantelides, and others, in which the linear index has been attributed to interionic transitions, i.e., the transfer of an electron from  $F^-$  to a  $Na^+$  ion in the NaF crystal.<sup>41</sup> This approach has considerable merit since the lowest-energy interband transitions are known to be of this nature, and therefore these transitions must be a major source of the polarizability. Pantelides has shown that the linear index can be calculated from

$$n^2 - 1 = Ad^3, \quad (12)$$

where  $d$  is the interionic spacing, and  $A$  is dependent only on the cation and the crystal structure. While this model might, in principle, be useful, the limitation lies in the fact that materials with a common anion, such as NaF and  $CaF_2$ , remain unrelated to each other since they have different values of  $A$ . Another approach involves bond-charge calculations.<sup>42,43</sup> We do not believe that these complex calculations are required to gain a qualitative understanding of  $n_2$  for the materials of interest here.

The prevailing concept of ionic crystals is that of predominantly independent ionic constituents which do not form covalent bonds. Therefore, a model which retains the identity of the ionic constituents is preferable. Within this framework, it has become generally accepted by numerous authors that it is appropriate to allow the polarizability of the anion to vary depending on the particular crystal at hand, while taking the value for the cation to be a constant. This concept has been justified by quantum-mechanical calculations<sup>11,44-46</sup> as well as by the use of simple semiempirical calculations.<sup>47-49</sup> As we will show in the next section, this picture is quite useful for the description of the hyperpolarizability, since the anion contribution tends to dominate the overall value for nearly all ionic materials, obviating the need to consider the

cation hyperpolarizability at all. In addition, although the anion hyperpolarizability shows an even greater sensitivity than the linear polarizability to the nearest neighbors (NN's), a simple dependence on the NN separation, independent of the identity of the cation, can be obtained, provided that the cation does not have a filled or unfilled  $d$  shell that contributes to the optical polarizability.

It is important to remark that it is not our purpose to judge the relative merit of any of the models discussed above. We prefer the description of a variable anion (hyper)polarizability, with a fixed or negligible cation contribution, because it provides the simplest physical interpretation for our results at this stage.

### B. Halides

Consider first the case of the halide anions. From our  $n_2$  data on several alkali halides it is possible to obtain values of the anionic hyperpolarizability from Eq. (5), where we assume that  $\gamma^+ \ll \gamma^-$  and use the value of  $n_2$  averaged over the [100] and [110] polarizations. We use the Lorentz local field for  $f$ . The resulting values of  $\gamma^-$  are listed in the last column of Table V. Recently, Johnson, Subbaswamy, and Senatore<sup>11</sup> performed extensive calculations of  $\alpha$  and  $\gamma$  for the anions and cations in the alkali halides. Their results for the in-crystal cation (+) and anion (-) contributions are also shown in Table V. These values were obtained from a self-consistent local-density-approximation (LDA) calculation of the energy of the ions in the applied electric field, and the interactions with the neighboring ions were modeled by pseudopotentials. The  $\alpha_c = \alpha^+ + \alpha^-$  values agree well with experiment. The hyperpolarizabilities  $\gamma = \gamma^+ + \gamma^-$  also agree reasonably well with our experimental data,

TABLE V. Comparison of the measured and theoretical hyperpolarizabilities (Hyperpol.) of the alkali halides.

Sample	Polarizability ( $\text{\AA}^3$ )		Hyperpol. ( $10^{-39}$ esu)		Comparison with experiment at $1.06 \mu\text{m}$	
	$\alpha^+$	$\alpha^-$	$\gamma^+$	$\gamma^-$	$\gamma^{\text{theory}}$ <sup>a</sup> (adjusted)	$\gamma^{\text{expt}}$
LiF	0.032	0.848	0.17	240.0	257.0	141.0
NaF	0.158	1.13	3.61	518.0	563.0	320.0
KF	0.839	1.28	62.4	780.0	906.0	889.0
RbF	1.39	1.38	174.0	1014.0		
LiCl	0.032	2.81	0.17	1210.0		
NaCl	0.158	3.26	3.55	2030.0	2380.0	1630.0
KCl	0.838	3.50	62.4	2750.0	3280.0	3050.0
RbCl	1.39	3.68	174.0	3444.0		
LiBr	0.032	3.86	0.17	2030.0		
NaBr	0.158	4.40	3.55	2750.0	4000.0	3370.0
KBr	0.838	4.66	61.8	4190.0	5240.0	4930.0
RbBr	1.39	4.89	172.0	5220.0		
LiI	0.032	5.67	0.17	3780.0		
NaI	0.159	6.37	3.55	5790.0		
KI	0.838	6.68	61.2	7260.0		
RbI	1.38	6.95	170.0	8820.0		

<sup>a</sup> The theoretical values were obtained from Ref. 12 and are extrapolated to  $\lambda = 1.06 \mu\text{m}$  using their formula.

considering the uncertainties in absolute calibration of the experimental results. The *relative* values differ from the experimental ratios quite substantially, particularly for the fluorides. For example, the measured value of  $\gamma$  for  $F^-$  varies by a factor of 6 as the cation size increases from Li to K, whereas a factor of 3.5 is obtained from the calculations. In view of the many experimental and theoretical difficulties involved, however, we consider the similar magnitudes of the *absolute* values in Table V to be very encouraging. We note that the frequency dependence for the theoretical values must be accounted for since they are calculated for  $\omega=0$ . This correction has been applied, as discussed in Ref. 12, although the changes were found to be small.

The calculations of Johnson *et al.* provide important insight into the origin and nature of  $\alpha$  and  $\gamma$ . From Table V we see that  $\alpha^+$  is nearly the same for a given cation, regardless of the halide ion involved. Similarly,  $\gamma^+$  also remains nearly constant. This means that the cation wave function is not strongly affected by the particular crystalline environment. In fact, the in-crystal values are nearly the same as the free-space values. On the other hand, the magnitudes of both  $\alpha^-$  and  $\gamma^-$  are observed to change substantially depending on the environment. For instance, for the LiF, NaF, KF, RbF series, the total relative change of  $\alpha^-$  is about 50%. For this same series,  $\gamma^-$  changes by a factor of 4. Although both  $\alpha^-$  and  $\gamma^-$  change depending on the crystal, the variation for  $\gamma^-$  is a good deal larger.

Johnson *et al.* have interpreted these results by suggesting that the anionic wave functions are being compressed by the repulsive potential of the surrounding cations. This repulsive potential decreases with increasing cation radius. As a result, the largest values of  $\gamma^-$  (or  $\alpha^-$ ) are observed for the crystal with the largest lattice constant. Another major difference between the trends exhibited by  $\alpha$  and  $\gamma$  is that the cationic contribution to the hyperpolarizability is negligible, while the values of  $\alpha^+$  and  $\alpha^-$  are similar. As we shall see, the fact that  $\gamma$  is determined almost entirely by  $\gamma^-$  greatly simplifies the interpretation of our data.

The basic differences between  $\alpha$  and  $\gamma$  can be rationalized by use of a simple expression,<sup>5</sup> in which it is assumed that all of the intermediate states are at the same energy  $E_0$ , and the light wave-frequency  $\omega \ll E_0/h$ ,

$$\alpha = \frac{2e^2}{E_0} \langle r^2 \rangle, \quad (13)$$

where  $\langle r^2 \rangle$  is the mean square distance of the electron from the nucleus. The analogous expression for the hyperpolarizability is

$$\gamma = \frac{48e^4}{E_0^3} (\langle r^4 \rangle / 2 - \langle r^2 \rangle^2). \quad (14)$$

The important difference in these expressions is that  $\alpha$  depends on  $\langle r^2 \rangle$ , while  $\gamma$  depends on  $\langle r^4 \rangle$  as well. This explains why  $\gamma^-$  is much more sensitive than  $\alpha^-$  to the identity of the nearest-neighbor cations, which perturb the anion wave functions at large values of  $r$ .

We can gain further insight into the data of Table V by

considering the model of Wilson and Curtis,<sup>47</sup> in which the polarizability is given by

$$\alpha^- = \alpha_0^- \exp(-C/R^2), \quad (15)$$

where  $R$  is the NN distance. This formula is obtained from a semiclassical argument based on the perturbation of the anion polarizability by the repulsive potential of the cations. In this model,  $\alpha_0^-$  is interpreted as the free-ion polarizability of the anion, and  $C$  is a measure of the sensitivity of the halide wave function to the NN cations. A comparison of the behavior predicted by this model with the values of  $\alpha^-$  for alkali halides calculated by Johnson *et al.*<sup>12</sup> is shown in Fig. 4(a), where the calculated  $\alpha^-$  from Table V are plotted as  $\ln \alpha^-$  versus  $R^{-2}$ . The fitted values of  $\alpha_0^-$  and  $C$  are given in Table VI. The value of  $C$  varies with increasing anion size from 3.87 for fluorides to 5.41 for iodides. Similarly, the magnitude of  $\alpha_0^-$  is observed to increase for the heavier halides.

In order to develop an analogous expression for the hyperpolarizability, Eqs. (13) and (14) are combined to give

$$\gamma = \frac{12}{E_0} (\langle r^4 \rangle / 2 \langle r^2 \rangle^2 - 1) \alpha^2. \quad (16)$$

If it is now assumed that  $E_0$  and  $\langle r^4 \rangle / \langle r^2 \rangle^2$  remain constant for a given halide series, Eq. (15) can be used to obtain the result

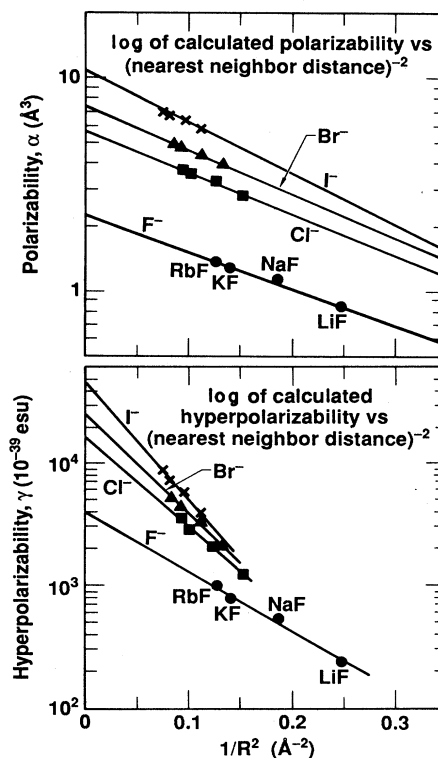


FIG. 4. Calculated anion polarizabilities (upper frame) and hyperpolarizabilities (lower frame) plotted as a function of  $R^{-2}$ , where  $R$  is the nearest-neighbor distance. The calculated values are from Ref. 12.

TABLE VI. Fitted parameters to the Wilson-Curtis empirical model [see Eqs. (15) and (17)].

Sample	Extrapolated free-ion polarizability $\alpha_0$ ( $\text{\AA}^3$ )		Extrapolated free-ion hyperpol. $\gamma_0$ ( $10^{-39}$ esu)		Slope $D$	
	Theor. <sup>a</sup>	Slope $C$ Theor. <sup>a</sup>	Theor. <sup>a</sup>	Expt. <sup>b</sup>	Theor. <sup>a</sup>	Expt. <sup>b</sup>
F <sup>-</sup>	2.24	3.87	4040	4950	11.3	14.7
Cl <sup>-</sup>	5.50	4.36	16 100		16.9	
Br <sup>-</sup>	7.24	4.66	24 400		18.6	
I <sup>-</sup>	10.5	5.41	47 500		22.6	
O <sup>2-</sup>				34 270		18.3

<sup>a</sup> See Fig. 4 and Ref. 12.

<sup>b</sup> This work.

$$\gamma^- = \gamma_0^- \exp(-D/R^2), \quad (17)$$

where it is predicted that  $D=2C$ . We have plotted the theoretical values of  $\gamma^-$  from Table V in the form of  $\ln\gamma^-$  versus  $R^{-2}$  in Fig. 4(b); the resulting values of  $D$  and  $\gamma_0$  are listed in Table VI in the column identified as "Theor." The average value of  $D/C$  is 3.7. If the Wilson-Curtis model holds exactly, and the prefactor of Eq. (16) is constant within each halide series, this ratio would be  $D/C=2$ . The considerable discrepancy from this value indicates that this model is too simple to account for the quantitative relationship between  $\alpha^-$  and  $\gamma^-$ . Figure 4 shows that the Wilson-Curtis model for anion polarizabilities, and its extension to hyperpolarizabilities, give a convenient parametrization of the calculations of Johnson *et al.*<sup>12</sup> for alkali halide crystals.

It is also interesting to compare fluorine and oxygen hyperpolarizabilities obtained from our measurements of  $n_2$  for various crystals with the Wilson-Curtis model. By use of the assumption that the anionic hyperpolarizability dominates the total value, the experimental values of  $\gamma^-$  for fluorine have been calculated from the  $n_2$  data using Eq. (5). These are given in Table VII in units of  $10^{-39}$  esu per fluoride ion. The NN distances are also listed. These experimental values of  $\ln\gamma^-$  are plotted versus

TABLE VII. Experimental neutral-formula-unit hyperpolarizabilities (Hyperpol.) for fluorides.

Neutral formula unit $M_xF$	Anion-cation <sup>a</sup> separation ( $\text{\AA}$ )	Hyperpol. $\gamma(M_xF)$ ( $10^{-39}$ esu)
LiF	2.01	141
NaF	2.32	320
KF	2.67	889
Mg <sub>1/2</sub> F	1.99 <sup>b</sup>	128
Ca <sub>1/2</sub> F	2.37	282
Sr <sub>1/2</sub> F	2.51	412
Cd <sub>1/2</sub> F	2.33	1520
Ba <sub>1/2</sub> F	2.69	626
La <sub>1/3</sub> F	2.50 <sup>c</sup>	487
Ce <sub>1/3</sub> F	2.48 <sup>d</sup>	440

<sup>a</sup> Reference 50.

<sup>b</sup> Reference 51.

<sup>c</sup> Reference 52.

<sup>d</sup> Extrapolated from LaF<sub>3</sub> by correcting for density.

$R^{-2}$  in Fig. 5. With the exception of CdF<sub>2</sub>, all of the data points lie on a line, the slope and intercept of which are given in Table VI. The interesting result here is that the values of  $D$  and  $\gamma_0$  are nearly the same as those determined from the alkali fluoride calculations of Johnson *et al.*; the experimental and theoretical values at 11.3 and 14.7  $\text{\AA}^2$  for  $D$ , and 4040 and 4950 ( $10^{-39}$  esu) for  $\gamma_0$ . It is important to note that the coordination of the fluorine ions differs considerably for the crystals from which these hyperpolarizabilities were obtained. For example, each F<sup>-</sup> is coordinated by six alkali cations in the alkali fluorides, and by a tetrahedron of cations in the alkaline-earth fluorides. It appears that the model in which the anionic wave functions are compressed by the NN cations, thereby reducing the hyperpolarizability, gives a good account of both  $\alpha^-$  and  $\gamma^-$ . In fact, the parameters in the model are somewhat independent of the cation and the crystal structure.

The anisotropy of  $n_2$  also provides evidence of the effects of the neighboring cations on the anion wave functions. We have used Eq. (9) to obtain the ratio  $r = \chi_{1122}^{(3)} / \chi_{1111}^{(3)}$  for numerous cubic crystals, and the results are given in Table VIII. The condition of isotropy (a value of  $n_2$  independent of polarization direction) is that  $r = \frac{1}{3}$ . For  $r > \frac{1}{3}$ , the value of  $n_2$  for light polarized

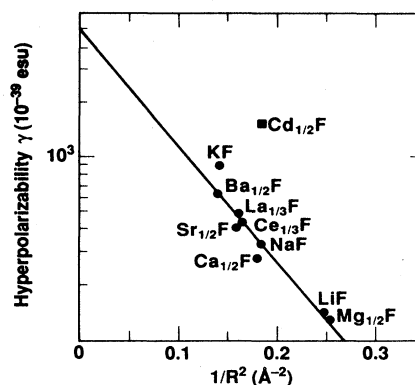


FIG. 5. Measured hyperpolarizability per fluorine ion plotted as a function of  $R^{-2}$  for some binary fluorides with various crystal structures. The square point was not included in the fit to Eq. (17).

along [110] is greater than along [100], and vice versa. From Table VIII we see that  $r=0.46$  for LiF, 0.45 for NaF, and 0.29 for KF. This behavior is in agreement with the idea of the compression of the halide wave function by the cations, since this compression would be greatest along [100], the direction of the fluorine-cation axis. It seems reasonable that the values of  $r$  should decrease for larger cations, since they have less overall effect on the fluorines due to the larger NN distance. A similar trend is found for NaCl and KCl. The larger errors associated with the bromides make the comparison more difficult. We briefly note that the oxides having the rocksalt structure, MgO and CaO, behave in the same manner as the halides.

The anisotropies of the fluorite-structure crystals deserve a separate discussion. Since each  $F^-$  is surrounded by a tetrahedron of divalent metal ions, the compression of the  $F^-$  wave function is very asymmetric, and it is difficult to determine the direction of maximum hyperpolarizability in any simple way. In Table VIII,  $r=0.56$  for  $CaF_2$ , 0.60 for  $SrF_2$ , and 0.66 for  $BaF_2$ . The value for  $CdF_2$ , 0.31, is completely out of line, since the lattice constant of  $CdF_2$  is nearly the same as that of  $CaF_2$ . Recalling from Fig. 5 that  $\gamma^-$  for  $CdF_2$  is far above the line that fits the other fluorides, it is clear that the hyperpolarizability of  $CdF_2$  has a fundamentally different origin. Ions like Cd with high-lying, filled outer  $d$  shells will be discussed separately.

### C. Oxides and sulfides

In Table IX are listed some oxygen hyperpolarizabilities per  $M-O$  formula unit. Most of these are calculated directly from the measured  $n_2$  for a number of simple oxide crystals using Eq. (5), assuming that the cation hyperpolarizabilities are negligible. The values for BeO and  $Sc_{2/3}O$  were obtained from  $BeAl_2O_4$  and  $Gd_3Sc_2Al_3O_{12}$

TABLE IX. Experimental neutral-formula-unit hyperpolarizabilities (Hyperpol.) for oxides and sulfides.

Neutral formula unit $M_xO, M_xS$	Anion-cation <sup>a</sup> separation (Å)	Hyperpol. $\gamma(M_xO < M_xS)$ ( $10^{-39}$ esu)
BeO	1.65	436.0 <sup>b</sup>
MgO	2.11	485.0
CaO	2.41	1500.0
ZnO	1.98	4850.0
SrO	2.58	2290.0
$Al_{2/3}O$	1.91	248.0
$Sc_{2/3}O$	2.11	920.0
$Ga_{2/3}O$	2.00	887.0
$Y_{2/3}O$	2.27	945.0
$Er_{2/3}O$	2.26 <sup>c</sup>	1040.0 <sup>d</sup>
fused $Si_{1/2}O$	1.61	510.0
$Ti_{1/2}O$	1.96	2520.0
$Zr_{1/2}O$	2.26	650.0
ZnS	2.34	8420.0
CdS	2.53	57 000.0

<sup>a</sup> Reference 51.

<sup>b</sup> Obtained from  $BeAl_2O_4$  and  $Al_2O_3$  assuming additivity.

<sup>c</sup> Obtained from  $Y_2O_3$  by correcting for density.

<sup>d</sup> We have assumed  $Er_{2/3}O$ ,  $Gd_{2/3}O$ ,  $La_{2/3}O$ , and  $Lu_{2/3}O$  have the same hyperpolarizability.

using the additivity assumptions to be discussed in subsection D. The cation- $O^{2-}$  separations are also given. The most significant property of these results is that the oxygen hyperpolarizability varies by about an order of magnitude from  $Al_2O_3$  to  $TiO_2$ . A plot of  $\ln \gamma^-$  versus  $R^{-2}$  is shown in Fig. 6. In contrast to the fluoride data, substantial scatter is observed, although the  $M-O$  pairs (rounded data points) that are ionic in character and for which the cation does not have filled or unfilled  $d$ -

TABLE VIII. Anisotropy of  $\chi^{(3)}$  of cubic crystals.

Sample	$n_2^a$ ( $10^{-13}$ esu)	$\chi_{1122}/\chi_{1111}^{b,c}$	$\chi_{1122}/\chi_{1111}$
LiF	0.26	0.460±0.017	0.45±0.06 <sup>d</sup>
NaF	0.34	0.447±0.012	
KF	0.75	0.293±0.024	
NaCl	1.59	0.373±0.013	0.43 <sup>d</sup>
KCl	2.01	0.303±0.013	0.30 <sup>d</sup>
NaBr	3.26	0.424±0.064	
KBr	3.07	0.449±0.127	0.37 <sup>d</sup>
$CaF_2$	0.43	0.556±0.020	0.50 <sup>d</sup> , 0.44±0.12 <sup>e</sup>
$SrF_2$	0.50	0.598±0.025	0.68±0.09 <sup>e</sup>
$CdF_2$	3.95	0.307±0.010	0.32±0.05 <sup>e</sup>
$BaF_2$	0.67	0.658±0.008	0.66±0.01 <sup>e</sup>
MgO	1.6	0.482±0.025	0.546 <sup>d</sup>
CaO	5.07	0.262±0.028	

<sup>a</sup> Polarization along [100], propagate down [001] axis.

<sup>b</sup> Assume  $\chi_{1122}^{(3)} = \chi_{1221}^{(3)}$ .

<sup>c</sup> Results from this work.

<sup>d</sup> Reference 2.

<sup>e</sup> Reference 23.

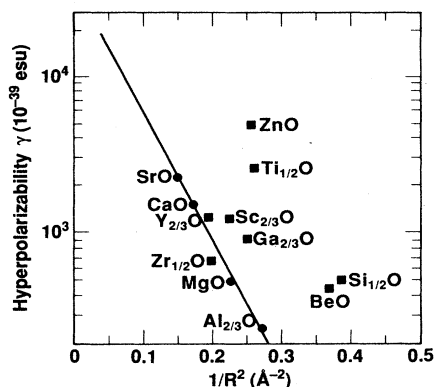


FIG. 6. Measured hyperpolarizability per oxygen ion plotted as a function of  $R^{-2}$  for some binary oxides with various crystal structures. The square points were not included in the fit to Eq. (17).

electron states in their outer shells can be fitted well by the line shown in the figure. From the slope of this line, the value of  $D = 18.29$  is obtained, which is quite similar to the value of 14.7 determined from the fluorides in Fig. 5 and Table VI. A major difference between  $F^-$  and  $O^{2-}$  is the value of  $\gamma_0$  which is (in  $10^{-39}$  esu) 34 270 for  $O^{2-}$  and 4950 for  $F^-$ . This reflects the much higher average hyperpolarizability of oxygen.

We briefly consider the data points of Fig. 6 that lie far from the line. It is likely that the Wilson-Curtis model requires that the metal-oxygen pairs that are fitted by the same values of  $D$  and  $\gamma_0$  have similar degrees of ionicity, similar types of low-lying excited states that can be occupied by the  $O^{2-}$  electrons in response to the optical field, and no valence-band states derived primarily from the occupied shells of the cation.  $Ti^{4+}$ ,  $Sc^{3+}$ , and other transition-metal ions with empty or sparsely occupied  $d$ -shells provide conduction-band states derived from both their outer  $d$  and  $s$  shells. They therefore differ in a fundamental way from cations with stable, rare-gas configurations, such as the alkali metals, alkaline-earth metals, rare-earth metals, and some other common cations ( $Al^{3+}$  and  $B^{3+}$ ). The very large hyperpolarizabilities of the  $Ti_{1/2}O$  and  $Sc_{2/3}O$  pairs can therefore be attributed to the large number of low-lying, empty  $3d$  states of these cations. Cations with filled outer  $d$  shells ( $Cu^+$ ,  $Ag^+$ ,  $Au^+$ ,  $Zn^{2+}$ ,  $Cd^{2+}$ ,  $Hg^{2+}$ ,  $Ga^{3+}$ , etc.) may, on the other hand, greatly augment the effective number of valence electrons.<sup>53</sup> In  $CdF_2$ , for example, the  $4d^{10}$  states of  $Cd^{2+}$  lie within a few eV of the  $2p$  states of the fluoride ion.<sup>54</sup> This accounts for the anomalously large effective hyperpolarizability for the  $Cd_{1/2}F$  pair in Fig. 5. It is likely that the number of anomalously large fluorine hyperpolarizabilities in Fig. 5 would be much larger if more transition-metal fluorides had been measured. Finally, we briefly mention some of the oxide crystals which appear toward the end of Table IV. These materials contain oxide ions in "complexes," such as  $CO_3^{2-}$ ,  $PO_4^{3-}$ , and  $WO_4^{2-}$ . The oxygens are so strongly covalently

bound to the central metal ion that, in actuality, the  $O^{2-}$  ion cannot be approximated as an independent entity at all.

Lastly, we mention the two sulfides for which we have data,  $ZnS$  and  $CdS$ . The anion hyperpolarizabilities of  $ZnO$  and  $ZnS$  are 4850 and 8420, respectively, in  $10^{-39}$  esu (see Table IX). Since these materials are both covalently bound and have identical lattice structure, this comparison should be meaningful, and gives an indication that sulfides are, in general, expected to have somewhat larger nonlinear indices than oxides.

#### D. Additivity of hyperpolarizabilities

It is interesting to examine whether the hyperpolarizabilities given in Table IX can be employed to calculate the nonlinear indices of other compounds of these constituents. A precedent for this with regard to linear-optical properties is the work of Gladstone and Dale,<sup>55</sup> who studied mixtures of liquids. Subsequently, Mandarino<sup>56-59</sup> used the refractive indices of simple compounds to calculate the indices for more complex compounds that contained the same elements. If we regard the results in Tables V, VII, and IX as cation-anion-pair hyperpolarizabilities,  $\gamma_i$ , which are simply additive, then the nonlinear refractive index of any compound containing these constituents can be calculated from Eq. (5) by summing over these pairwise hyperpolarizabilities, where  $N_i$  is the number of each per unit volume, and  $f$  is assumed to be the Lorentz local-field factor. The results of such a scheme are shown in Table X for a number of complex oxide crystals. The agreement is very good; the average error is about 13%. This result is more significant than it may seem, because the cations in these complex oxides have, in several cases, different oxygen coordinations than in the simple oxide, and each oxygen is coordinated by up to three different cations. For example, in the garnet structure Al or Ga can be both octahedrally and tetrahedrally coordinated, and each oxygen is coordinated by one rare-earth ion and two transition-

TABLE X. Nonlinear index values calculated using additivity of hyperpolarizabilities (listed in Table VII).

Sample	$n$ (1.06 $\mu\text{m}$ )	$n_2$ ( $10^{-13}$ esu) measured	$n_2$ ( $10^{-13}$ esu)
			calculated from simple oxides
BeAl <sub>2</sub> O <sub>4</sub> <sup>a</sup>	1.73	1.46	
MgAl <sub>2</sub> O <sub>4</sub>	1.72	1.50	1.3
CaMgSi <sub>2</sub> O <sub>6</sub>	1.67	1.73	2.2
YAlO <sub>3</sub>	1.93	3.37	4.8
Y <sub>3</sub> Al <sub>5</sub> O <sub>12</sub>	1.82	2.7	3.0
Gd <sub>3</sub> Sc <sub>2</sub> Al <sub>2</sub> O <sub>12</sub> <sup>a</sup>	1.89	4.0	
Gd <sub>3</sub> Sc <sub>2</sub> Ga <sub>3</sub> O <sub>12</sub>	1.94	5.5	5.7
Gd <sub>3</sub> Ga <sub>5</sub> O <sub>12</sub>	1.94	5.8	5.2
Y <sub>3</sub> Ga <sub>5</sub> O <sub>12</sub>	1.91	5.2	5.5
La <sub>3</sub> Lu <sub>2</sub> Ga <sub>3</sub> O <sub>12</sub>	1.93	5.8	5.4
SrTiO <sub>3</sub>	2.31	26.7	30.0

<sup>a</sup>  $\gamma$  for BeO and  $Sc_{2/3}O$  extrapolated from these materials.

metal ions. Even under those conditions, the limited results that we have so far obtained suggest that the additivity of hyperpolarizabilities of cation-oxygen pairs is a reasonably good approximation.

#### E. Choice of local-field correction

The presence of the fourth power of the local-field correction  $f$  in Eq. (5) suggests that the particular choice for  $f$  is very important. The Lorentz local field is rigorously applicable only to the case of highly localized electrons in a cubic lattice. These conditions are not satisfied in many of our samples. We have investigated this point by ignoring the local-field correction in Eq. (5) and by rederiving the BGO formula assuming that  $f = 1$ . The modified BGO formula gives a fit to the measurements that is not very different from that shown in Fig. 4, in which the calculated values were obtained using the original BGO formula in Eq. (6). If the local-field correction is ignored in determining the oxygen hyperpolarizabilities in Table IX from the data on simple oxide crystals, the values of the hyperpolarizabilities are, of course, different. If, however, these new hyperpolarizabilities are used to calculate the values of  $n_2$  in Table X, again using  $f = 1$ , there is still reasonable agreement with the measurements; the average error increases to 17%, compared with 13% using the Lorentz local field. We conclude that there is really very little that can be learned from the  $n_2$  measurements about the best choice of local-field correction.

#### V. CONCLUSIONS

We have shown that relative values of  $n_2$  can be measured with an accuracy of about 5% using nearly degenerate three-wave mixing. The BGO empirical formula was found to predict  $n_2$  to within an average accuracy of about 30% for a variety of types of crystals, with  $n_2$  values ranging over 3 orders of magnitude. A new value,  $K = 48$ , of the multiplicative constant in that formula was found to be optimum for the full set of crystals that were investigated. The BGO formula tends to overestimate the nonlinear index of some transition-metal oxides with

high linear refractive indices and it yields poor predictions of the anisotropy of  $n_2$  in uniaxial and biaxial crystals.

The recent calculations of Johnson *et al.*<sup>12</sup> for alkali halide crystals give generally good agreement with the halide ion hyperpolarizabilities obtained from our measurements, although the measured set of alkali halide crystals was not large enough to provide a thorough comparison. For fluorides and oxides of cations with stable rare-gas cores, our results show a good correlation between the effective anion hyperpolarizabilities,  $\gamma^-$ , and the nearest-neighbor distance, independent of crystal structure and coordination number of these anions. In general, cations with filled outer  $d$  shells and low-lying unoccupied  $d$  states give enhanced values of  $\gamma^-$ . The effective hyperpolarizabilities of the oxide and fluoride ions were found to vary by about a factor of 10 for the compounds that we measured.

The values of  $\gamma^-$  for the oxygen ion obtained from binary oxides were treated as anion-cation-pair hyperpolarizabilities, from which  $n_2$  values were calculated for more complex oxides containing two or more different cations. These calculated values are in good agreement with the measured values for a set of complex oxides with various crystal structures and coordination numbers for the oxygen ions. This formalism provides an alternative to the BGO formula for predicting  $n_2$  for materials, particularly where there is no linear-refractive-index data available.

#### ACKNOWLEDGMENTS

We wish to thank M. D. Johnson and K. R. Subbaswamy for helpful discussions and for communicating the results of their calculations prior to publication, L. A. Boatner and L. G. DeShazer for the loan of numerous crystals, E. Prochnow for polishing many of our samples, and G. Smith for x-ray orientation of the crystals. This research was performed, under the auspices of the Division of Materials Sciences of the Office of Basic Energy Sciences, U.S. Department of Energy, by Lawrence Livermore National Laboratory under Contract No. W-7405-ENG-48.

<sup>1</sup>Y. R. Shen, *The Principles of Nonlinear Optics* (Wiley, New York, 1984).

<sup>2</sup>P. D. Maker and R. W. Terhune, *Phys. Rev.* **137**, A801 (1965).

<sup>3</sup>R. C. Miller, *Appl. Phys. Lett.* **5**, 17 (1964).

<sup>4</sup>C. C. Wang, *Phys. Rev. B* **2**, 2045 (1970).

<sup>5</sup>N. L. Boling, A. J. Glass, and A. Owyong, *IEEE J. Quantum Electron.* **QE-14**, 601 (1978).

<sup>6</sup>A. Yariv, *Quantum Electronics*, 2nd ed. (Wiley, New York, 1975), p. 499.

<sup>7</sup>W. L. Smith, in *Handbook of Laser Science and Technology*, edited by M. J. Weber (Chemical Rubber Co., Boca Raton, 1986), Vol. 3, Pt. 1, p. 259.

<sup>8</sup>A. Feldman, D. Horowitz, and R. M. Waxler, *IEEE J. Quantum Electron.* **QE-9**, 1054 (1973).

<sup>9</sup>R. A. Garaev, D. V. Vlasov, and V. V. Korobkin, *Kvantovaya*

*Elektron.* (Moscow) **9**, 155 (1982) [*Sov. J. Quantum Electron.* **12**, 100 (1982)].

<sup>10</sup>L. L. Boyle, A. D. Buckingham, R. L. Disch, and D. A. Dunmur, *J. Chem. Phys.* **45**, 1318 (1966).

<sup>11</sup>K. R. Subbaswamy and G. D. Mahan, *J. Chem. Phys.* **84**, 3317 (1986).

<sup>12</sup>M. D. Johnson, K. R. Subbaswamy, and G. Senatore, *Phys. Rev. B* **36**, 9202 (1987).

<sup>13</sup>J. R. Tessman, A. H. Kahn, and W. Shockley, *Phys. Rev.* **92**, 890 (1953).

<sup>14</sup>M. J. Moran, C.-Y. She, and R. L. Carmen, *IEEE J. Quantum Electron.* **QE-11**, 259 (1975).

<sup>15</sup>D. Milam and M. J. Weber, *J. Appl. Phys.* **47**, 2497 (1976).

<sup>16</sup>D. Milam and M. J. Weber, *Opt. Commun.* **18**, 172 (1976).

<sup>17</sup>D. Milam, M. J. Weber, and A. J. Glass, *Appl. Phys. Lett.* **31**,

- 822 (1977).
- <sup>18</sup>M. J. Weber, D. Milam, and W. L. Smith, *Opt. Eng.* **17**, 463 (1978).
- <sup>19</sup>R. Adair, L. L. Chase, and S. A. Payne, *J. Opt. Soc. Am. B* **4**, 875 (1987).
- <sup>20</sup>S. A. Akhmanov, L. B. Meisner, S. T. Parinov, S. M. Saltiel, and V. G. Tunkin, *Zh. Eksp. Teor. Fiz.* **73**, 1710 (1977) [*Sov. Phys.—JETP* **46**, 898 (1977)].
- <sup>21</sup>D. Heiman, R. W. Hellwarth, and D. S. Hamilton, *J. Non-Cryst. Solids* **34**, 63 (1979).
- <sup>22</sup>B. Hegemann and J. Jonas, *J. Chem. Phys.* **82**, 2845 (1985).
- <sup>23</sup>M. D. Levenson and N. Bloembergen, *Phys. Rev. B* **10**, 4447 (1974).
- <sup>24</sup>R. T. Lynch, Jr., M. D. Levenson, and N. Bloembergen, *Phys. Lett.* **50A**, 61 (1974).
- <sup>25</sup>M. D. Levenson, *IEEE J. Quantum Electron.* **QE-10**, 110 (1974).
- <sup>26</sup>S. R. Freiberg and P. W. Smith, *IEEE J. Quantum Electron.* **QE-23**, 2089 (1987).
- <sup>27</sup>W. L. Smith, J. H. Bechtel, and N. Bloembergen, *Phys. Rev. B* **12**, 706 (1975).
- <sup>28</sup>C. C. Wang, *Phys. Rev. B* **2**, 2045 (1970).
- <sup>29</sup>H. H. Li, *J. Phys. Chem. Ref. Data* **5**, 329 (1976).
- <sup>30</sup>M. J. Dodge, in *Handbook of Laser Science and Technology*, edited by M. J. Weber (Chemical Rubber Co., Boca Raton, 1986), Vol. 4, Pt. 2, Sec. 1.1.1.2.
- <sup>31</sup>S. Singh, in *Handbook of Laser Science and Technology*, edited by M. J. Weber (Chemical Rubber Co., Boca Raton, 1986), Vol. 3, Pt. 1, Sec. 1.1.
- <sup>32</sup>Gan Fu-Xi and Lin Feng-Ying, *Wuli* **8**, 385 (1979).
- <sup>33</sup>*Handbook of Chemistry and Physics*, 62nd ed., edited by R. C. Weast (Chemical Rubber Co., Boca Raton, 1981), Sec. B.
- <sup>34</sup>T. Marciov and K. Truszkowska, *Appl. Opt.* **20**, 1755 (1981).
- <sup>35</sup>*Handbook of Chemistry and Physics*, 38th ed., edited by Charles D. Hodgman (Chemical Rubber Co., Cleveland, 1956), p. 1423.
- <sup>36</sup>P. K. Tien, R. J. Martin, S. L. Blank, S. H. Temple, and L. J. Varrerin, *Appl. Phys. Lett.* **21**, 207 (1972).
- <sup>37</sup>S. A. Balabanova, E. V. Zharikov, V. V. Laptev, and V. D. Shigorin, *Kristallografiya* **29**, 1201 (1984) [*Sov. Phys.—Crystallogr.* **29**, 704 (1984)].
- <sup>38</sup>K. Enke and W. Tolksdorf, *Rev. Sci. Instrum.* **49**, 1625 (1978).
- <sup>39</sup>D. Eimerl (private communication).
- <sup>40</sup>For a recent review, see J. Shonker, G. G. Agrawal, and N. Dutt, *Phys. Status Solidi B* **138** (1986).
- <sup>41</sup>S. T. Pantelides, *Phys. Rev. Lett.* **35**, 250 (1975).
- <sup>42</sup>B. F. Levine, *Phys. Rev. B* **7**, 2600 (1973).
- <sup>43</sup>V. G. Tsirelson, O. V. Korolkova, I. S. Rez, and R. P. Ozerov, *Phys. Staus Solidi B* **122**, 599 (1984).
- <sup>44</sup>P. W. Fowler and P. A. Madden, *Phys. Rev. B* **29**, 1035 (1984).
- <sup>45</sup>G. D. Mahan, *Phys. Rev. B* **34**, 4235 (1975).
- <sup>46</sup>G. D. Mahan, *Solid State Ionics* **1**, 29 (1980).
- <sup>47</sup>J. N. Wilson and R. M. Curtis, *J. Phys. Chem.* **74**, 187 (1970).
- <sup>48</sup>H. Coker, *J. Phys. Chem.* **80**, 2078 (1976).
- <sup>49</sup>H. Coker, *J. Phys. Chem. Solids* **40**, 1079 (1979).
- <sup>50</sup>F. S. Galasso, *Structure and Properties of Inorganic Solids* (Pergamon, New York, 1970).
- <sup>51</sup>R. S. Shannon and C. T. Prewitt, *Acta Crystallogr.* **25**, 925 (1968).
- <sup>52</sup>W. T. Carnall, H. Carnall, and H. M. Crosswhite (private communication).
- <sup>53</sup>S. H. Wemple and M. Didomenico, *Phys. Rev. Lett.* **23**, 1156 (1969).
- <sup>54</sup>J. W. Hodby, *Crystals With the Fluorite Structure*, edited by W. Hayes (Clarendon, Oxford, 1974), p. 19.
- <sup>55</sup>J. H. Gladstone and T. P. Dale, *Philos. Trans. R. Soc. London* **153**, 317 (1864).
- <sup>56</sup>J. A. Mandarino, *Can. Mineral.* **14**, 498 (1976).
- <sup>57</sup>J. A. Mandarino, *Can. Mineral.* **16**, 169 (1978).
- <sup>58</sup>J. A. Mandarino, *Can. Mineral.* **17**, 71 (1979).
- <sup>59</sup>J. A. Mandarino, *Can. Mineral.* **19**, 441 (1981).